INPUT GROUND MOTION CALCULATION BASED ON DYNAMIC RUPTURE MODELING ON SEGMENTED FAULTS

H. Aochi[1]

[1]Bureau de Recherche Géologiques et Minières, Orléans, France

E-mail contact of main author: h.aochi@brgm.fr

Abstract. Since more than a decade, it has been shown that dynamic rupture modeling is able to reproduce the near-field ground motions as well as kinematic source models. Such approach is then taken into account for estimating probable earthquake scenarios in the recent research of seismic hazard study. The advantage of dynamic rupture modeling is that (1) the interaction between fault segments is considered, (2) the causality on the kinematic parameters such as rupture time, maximum slip velocity and slip is assured by mechanics, (3) the source time function is naturally provided as a result, and (4) the macroscopic fault parameter (maximum magnitude) can be discussed in the given fault system. Among various numerical methods available nowadays, a 3D Boundary Integral Equation Method is always useful in its portability and handiness. One typical scenario of magnitude 7 can be calculated in an hour on parallel computers. This paper aims to argue the important parameters during constructing a dynamic rupture model and review the example for the the 2007 Mw6.6 Niigata-Chuetsu-oki (Japan) earthquake is discussed.

Key Words: Fault segmentation, Fault geometry, Dynamic rupture process, Near-field ground motion .

1. Introduction

Quantitative and reliable ground motion estimation under a given context at a site of interest is a key technical issue for the engineering design of structures. Installation of important facilities requires detail time-series analyses of the resilience of the structures under probable ground shakings. Many empirical or stochastic methods have been operational, and sophisticated deterministic approaches are also considered (e.g. [1]). In the case that the site of interest is close to active faults (< a few tenths kilometers), the effect of this finite source should be taken into account in ground motion estimations, because we know from the past earthquakes that the rupture property characterizes significantly the ground motions and can lead to severe damages. For example, a guideline [2] is given how to construct a kinematic finite source model for ground motion calculations of engineering practices. Their approaches are based on the statistical characterization retrieved from the earthquake models of seismological kinematic inversions.

Since more than a decade, it has been shown that dynamic rupture modeling is also able to reproduce the near-field ground motions (e.g. [3, 4]) as well as kinematic source models. Such approach is then taken into account for estimating probable earthquake scenarios in the recent researches of seismic hazard study (e.g. [5]). The advantage of dynamic rupture modeling is that

(1) the interaction between fault segments is considered,

(2) the causality on the kinematic parameters such as rupture time, maximum slip velocity and slip is assured by mechanics,

(3) the source time function is naturally provided as a result, and

(4) the likelihood of the macroscopic fault parameter (maximum magnitude) can be discussed based on the mechanical insights in the given fault system.

The purpose of this short note is to give the practices of dynamic rupture simulations for engineering purpose, rather than to discuss the scientific topics. Parameter setting is essential and the most difficult part for the applications.

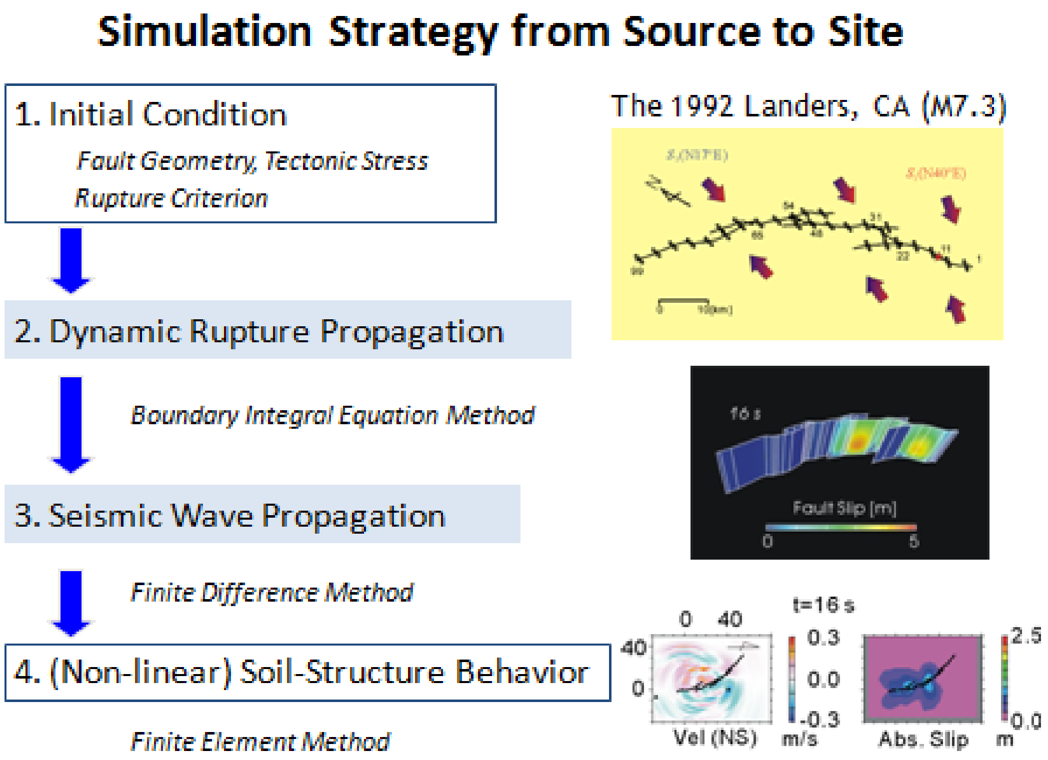

FIG. 1. Schematic illustration of "two-step" simulation, beginning with (1) the initial condition for (2) dynamic rupture process and (3) wave propagation. This can be coupled with further analyses of (4) soil and structure response at a site of interest.

2. Methodology

Here, we propose "two-step" simulation procedure from the dynamic rupture process to the ground motion simulation (FIG. 1) as originally applied in the forward modelings [6-9], and also commonly adapted in the dynamic inversions [10, 11]. The most important is the initial and boundary condition to drive the simulations. This paper proposes to take into account of the non-planar fault geometries, in which the ones should consider the absolute stress field in the medium. This is different from the case of any single planar fault for which only a relative change in stress appears. Once the fault geometry and the stress field are set, a small initial rupture is given at a chosen hypocenter, the rupture process goes on spontaneously according to a given rupture criterion and friction law with respect to the stress evolution, and the seismic waves are radiated.

In the 'two-step' simulation framework, we use a Boundary Integral Equation Method (BIEM [12]) for the first dynamic rupture part and a Finite Difference Method (FDM [6, 9]) for the second wave propagation part. Although one single simulation method can handle both the processes simultaneously, there are two advantages to distinguish them from the point of view of cost performance of computation and the utility of the intermediate result. Namely,

+ The rupture process concerns mainly along the fault segments and the surrounding medium, which is much smaller than the dimension of the resultant wave propagation. Thus, solving the elastodynamic equations only for the fault segments and the nearby medium is better in cost performance of computing, rather than calculating the full volume of the medium from the finite source to the site of interest. This is also because the numerical resolution required in the computation is different at source element and the outer medium grid.
+ The fact that the wave propagation is sequentially simulated means that one can easily give other derivative or alternative rupture scenario based on the original one. For example, we can modify the scaling parameters included in the rupture scenario (ex. magnitude), or add some more complexity (random high frequency generation) in rupture scenario.

On the other hand, we remark the limit of the 'two-step' procedure.

- It is difficult to correctly take into account if the medium complexity very nearby the fault segment influences the rupture process itself.

Indeed, the interaction of the rupture process in bi-material medium, in damaged zone or with the ground surface is still on-going research topics.

The choice of the above methods for each step is not exclusive. There are many other possibilities of the different combinations such as the finite difference for the dynamic rupture part and the discrete wavenumber method for the wave propagation part. The advantage of the proposed choice here is in the following;

+ The BIEM is flexible for the fault segmentation and irregular fault geometry, and also usually much faster than the other volumetric numerical methods, as the method formulation is specialized for a unit fault segment.
+ The FDM is one of the most convenient methods to calculate the wave propagation in a 3D volume, and pre-processing of the grids (meshing) is not necessary, as structural grids are usually adapted.

The detailed formulation of the BIEM used in this study is summarized in [12]. There have been many different formulations (time or Fourier domains, stress or slip integrand, etc.) since a few decades. Our formulation is specialized for the rupture problem along the fault segment, so that stress is expressed by the spatio-temporal convolution of the Green function and fault slip to make it easy to couple with any rupture criterion. The Green function can be analytically formulated and discretized for a 3D homoegeneous, infinite medium. One of the most popular version would be the one formulated for a planar fault in a 3D medium [13, 14]. As similar formulations to ours, the recent improvements have been brought for a half-space problem [15] and for different 2D/3D cases and discretizations [16].

On the other hand, the FDM also has a very long history. We adapt the forth-order staggered grid in space and the second-order in time [17-19]. The characteristics of the FDM used in this study are given in [9]. Any earthquake source models (dynamically simulated and kinematically constructed) can be introduced in the finite difference scheme as a series of seismic moment release (on stress tensor). There have been some derivatives of the method, such as the introduction of a partially rotated staggered grid [20, 21], which makes it easier to incorporate the boundary condition. A good performance of the collocated-grid scheme is illustrated with curvilinear coordinate by optimizing the dissipation errors [22].

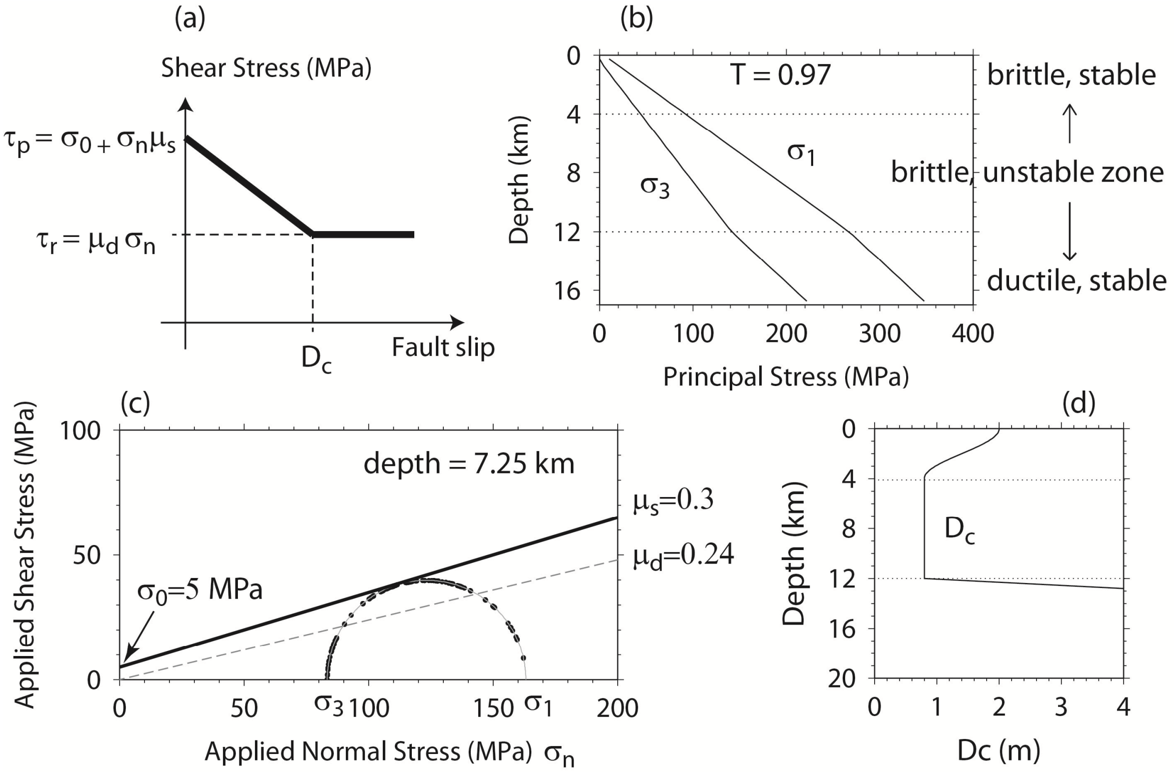

FIG. 2. (a) A typical linear slip-weakening law. (b) Depth variation of principal stresses σ_1 and σ_3 (both horizontally oriented) for strike-slip faulting regime. (c) Mohr circle with two Coulomb friction lines (static and dynamic) defined by μ_s and μ_d at a given depth. (d) Depth variation of Dc. See the text for detailed hypothesis. Modified after [27].

3. Best Practices for Parameter Setting

Reasonable parameter setting is a key of dynamic rupture modeling. This papers aims to give particular practices for a complex fault system of irregular geometry without taken into account of small scale heterogeneity on a single planar segment. Dynamic rupture modeling on a single planar fault has been long studied since 1970s (e.g. [23]) and this is always a good approximation of the causal earthquake source. The role of heterogeneity is important, as barriers, asperities and strong motion generation areas. In particular, randomness of the heterogeneity is discussed [24, 25], for example. Hereafter, as illustrated in FIG. 1, we consider the absolute stress field and a suitable rupture criterion (and friction law). If we think of a complete seismic cycle, the stress field before a characteristic earthquake of our interest should be somehow at a critical state, which is still difficult to be measured from the observation but can be estimated from some geodynamical seismic cycle simulations. This coupling becomes possible [26] in a realistic situation, but still needs much more researches for the practice and is beyond the focus of this paper. Thus, we should guess the initial state critical enough to begin a large earthquake.

For this purpose, as the first approximation, it is reasonable to assume that the fault system is embedded in a uniform stress field governed by principal stresses ($\sigma_1, \sigma_2, \sigma_3$ where $\sigma_1 \geq \sigma_2 \geq \sigma_3$). For a large earthquake of magnitude over 7, it is more plausible to consider some variation. Typically we suggest introducing a depth-variation, say for a type of shallow characteristic earthquakes, from a depth of 0 to 15 km. This reflects the fact that the confining pressure increases with depth, so that the stress field is naturally larger at depth. It is supposed that the directions of principal stress (thus, the type of fault mechanism) are known from prior information such as the regional tectonics or the focal mechanism analyses, and their values remain to decide.

Then, a Mohr-Coulomb rupture criterion and a linear slip-weakening friction are commonly used. We avoid writing all the equations, and illustrate a diagram in Figure 2 for a case of strike-slip faulting regime. The Mohr-Coulomb criterion is generally described by a static frictional coefficient μ_s and a cohesive force σ_0. A slip-weakening friction needs a dynamic frictional coefficient μ_d and a critical slip displacement D_c. We need to decide how the Mohr-circle is located in the two static and dynamic Coulomb friction lines. We introduce a scalar parameter T ($0 \leq T \leq 1$) [27] indicating how Mohr circle is close to the Coulomb friction lines, defined by

$$T = \left.\frac{\text{possible stress drop}}{\text{breakdown strength drop}}\right|_{\text{for optimal plane}} = \left.\frac{\sigma_0 + (\mu_s - \mu_d)\sigma_n}{\tau - \mu_d \sigma_n}\right|_{\text{for optimal plane}} . \qquad (1)$$

The case of T = 1 means that the circle tangentially touches the static Coulomb line, while for the other end member T = 0, it reaches only with the dynamic Coulomb line. One can suppose any negative T, but there is no interest for the dynamic rupture process, as there is no possibility of positive stress drop. The model parameters and its particular values used for illustrating FIG. 2 are summarized in Table 1. Implicitly the intermediate principal stress σ_2 (vertical) is supposed to be $(\sigma_1 + \sigma_3)/2$ and equal to the hydrostatic pressure at each depth. Below 12 km, a ductile feature of interface is expected due to high temperature, so a different relation (deviatric stress does not increase any more, and frictional evolution is plastic or hardening) is given. This detail is not less important for the dynamic rupture, and important is to know to what extent of depth the seismogenic zone continues.

From several modeling experiences of the past and scenario earthquakes, there are some recommendations:

- The frictional coefficient is smaller than the laboratory experiments of dry rock (0.6-0.7), but the occurrence of the past earthquakes in complex fault geometry prefers a 'weak' fault assumption with hydrostatic pressure and a moderate frictional coefficient (0.3-0.4). Otherwise, the rupture is not able to propagate (i.e. [28, 29]).
- Average stress drop is about several MPa, upto 10 MPa. For this, dynamic frictional coefficient is set as 70-80% of the static one. This signifies that a stress drop is about 1/5 – 1/4 of the absolute stress field.
- A cohesive force of several MPa is preferred, meaning the fault strength at depth 0. A zero cohesive force permits no stress accumulation and release, but a significant rupture is possible near the ground surface [30].

- Dc is given according to the scaling of the earthquakes, such that Dc is about 10 cm for a magnitude 6 (fault dimension of 10 km), 30 cm for M7, 1 m for M8, and so on [25]. Dc can also take into account of the depth variation (FIG 2d, eg. [30]) to express “brittle but stable” in the shallow (longer Dc), “brittle and instable” in the seismogenic zone, and “ductile and stable” in the depth (very long Dc, namely perfect plasticity with no stress drop).

TABLE I. MODEL PARAMETERS NECESSARY FOR DYNAMIC RUPTURE MODELING, AND THE VALUES USED FOR FIG. 2 (SCENARIO EARTHQUAKES ALONG THE NORTH ANATOLIAN FAULT, TURKEY [27]).

Parameter	Given Value for FIG. 2
Static frictional coefficient μ_s	0.3
Dynamic frictional coefficient μ_d	0.24
Cohesive force σ_0	5 MPa
Scalar parameter of stress accumulation T	0.97
Intermediate principal stress σ_2	123 MPa at 7.25 km
Max/min principal stresses σ_1, σ_3 (*)	163/83 MPa at 7.25 km

4. Applications – 2007 Mw6.6 Niigata-Chuetsu-oki Earthquake

We show an example of the dynamic rupture simulation and the estimation of the near-field ground motion for the 2007 Mw6.6 Niigata-Chuetsu-oki, Japan, earthquake (FIG. 3). This led to the shutdown of the Kashiwazaki-Kariwa nuclear power plant near-by (denoted as station KSH) and influenced the seismic safety approaches of nuclear installations [31]. Strong ground motions (stronger than the ones used for designing the installations) were recorded at the site. In order to explain the observed strong pulses, the earthquake models are proposed consisting of three asperities located on a single SE dipping reverse fault [32], and they are reconstructed dynamically by adjusting frictional parameters [8] (Models AD2 and AD3 in FIG. 3). The asperities have twice the stress drop (-16 MPa) of the other part (-8 MPa) of the fault, and Dc is supposed 50 cm and 30 cm, respectively. Model AD2 represents concentric rupture propagation from the hypocenter (uniform in fault peak strength τ_p), while AD3 has an opposite rupture directivity on the third asperity, which can be realized by a rupture detour around a barrier (denoted by thick black lines). On the other hand, the dynamic rupture process on conjugate fault segments are simulated, namely the rupture starts on a NW dipping fault and transfers on a SE dipping conjugate one [9]. A parameter set (μ_s = 0.3, Dip angle of segment 2 = 45°, Overlapping of two segments = 4 km from [9]) is represented as Model AK in FIG. 3. Unlike the previous two models, each segment is expressed uniform. The hypocenter positions are set to (138.624°E, 37.5386°N, 8 km), noting an initial crack has a radius of a few kilometers in the dynamic rupture simulations. All these dynamic rupture models are simulated with the BIEM. The planar fault models (AD2 and AD3) could be calculated easily with other methods, while the conjugate fault model (AK) remains difficult, even if each segment is planar. If we knew a more detailed structure of the fault system, the model could be more complex. However it is still difficult to image precisely the buried fault structure.

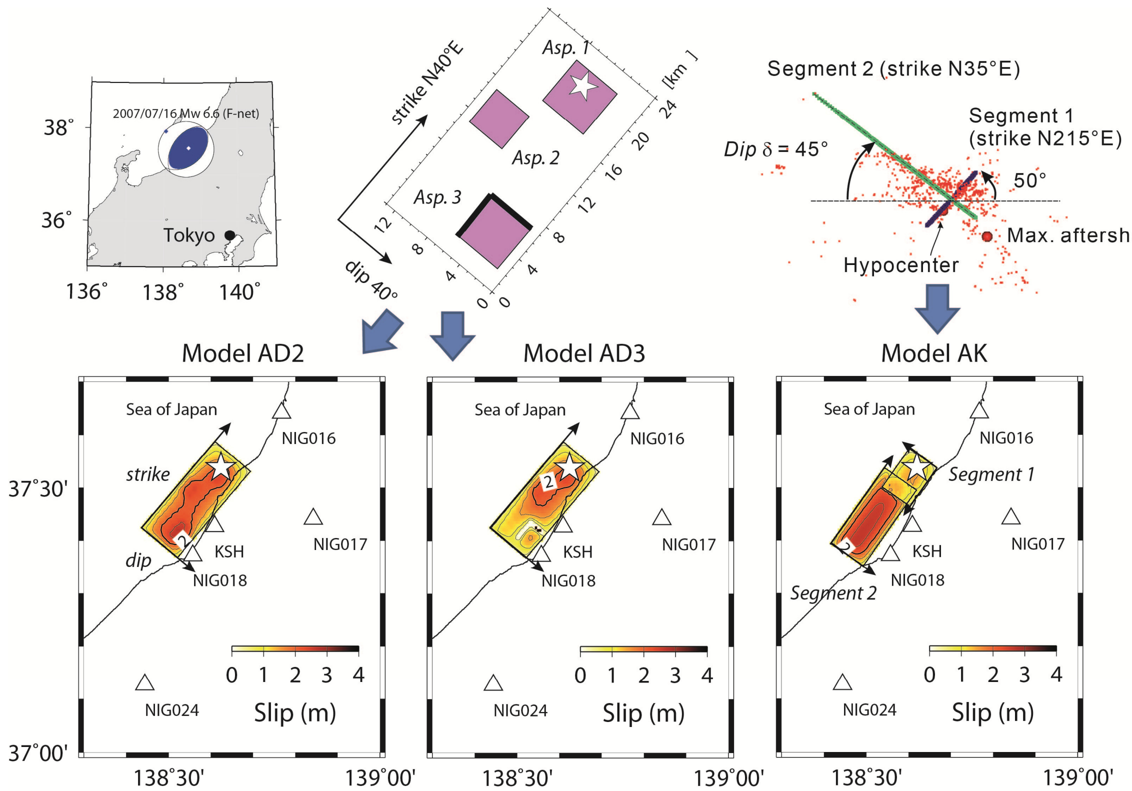

FIG. 3. Earthquake source models for the 2007 Niigata-chuetsu-oki earthquake. A SE dipping fault with three asperities (AD2 and AD3 [8]). The third asperity of AD3 is semi-surrounded by barrier (thick black lines) so that the rupture directivity is locally opposite. A conjugate segmented fault model with different dipping directions (AK [29]). The stars represent the hypocenter position. The triangles show the seismic stations.

These dynamic source models are put in the wave propagation simulations using the FDM, as previously different kinematic source models are tested in various available 3D geological models [33]. Here we use the structure model calibrated by Geological Survey of Japan [34]. We set a minimum wave velocity at 800 m/s for a grid size of 100 m. A snapshot of the ground motion in a homogeneous model is shown in [8] to clarify the difference of such three dynamic models in the radiated waves. A strong wave front propagates commonly towards the south-west direction due to the rupture directivity. Besides we find another wave front heading to the east in AD3 and AK models due to the significant change in rupture geometry. FIG. 4 shows a comparison of the ground motion at four stations, NIG016, NIG017, NIG024 (at ground surface) and KSH (at the service hall at depth of 250 m, SG4). Even if no significant heterogeneity exists in slip distribution, some characteristics of the near-field ground motions (NIG016, NIG017 and NIG024) are captured in its frequency content and in significant phases. In the forward direction (NIG024), the waveforms are mainly represented by the propagation of the rupture front and its arrest, and there are few differences among the models. At the side (NIG017 and KSH), more phases can be recognized due to the local change of rupture behavior. As no tuning or no inversion was carried out at this step, it is difficult to compare visually the seismograms. It has been proposed to evaluate the synthetic ground motions through the ground motion parameters such as peak ground acceleration, velocity and displacement, duration, Arias intensity, response spectra [35, 36] rather than the waveforms usually used in seismology. This is because the engineering purpose is not always fitting the waveforms coherently. Therefore we apply a goodness-of-fit (GOF) criterion [37], which can give a rough idea how two seismograms are close in envelope and phase. GOF score is briefly understood as excellent (8 < GOF < 10), good (6 < GOF < 8), fair (4 < GOF < 6) and poor (0 < GOF < 4). FIG. 5 shows time-frequency envelope goodness-of-fit diagrams for KSH. Model AK remains a better model among the three, by improving the GOF score in the NS component.

The example of the 2007 Chuetsu-oki earthquake presented in this session is not for calibrating the model parameters perfectly through inversion but for evaluating the performance of the input ground motion simulations based on the forward dynamic rupture modeling. Although each model could be improved, a GOF indicates a favorable score for the model AK consisting of the conjugate fault segments. This means that the complex ground motion can be the result from the perturbation in the dynamic rupture process, especially due to the irregular fault geometry. A more discussion is given on the comparison between kinematic and dynamic rupture models for this earthquake [38].

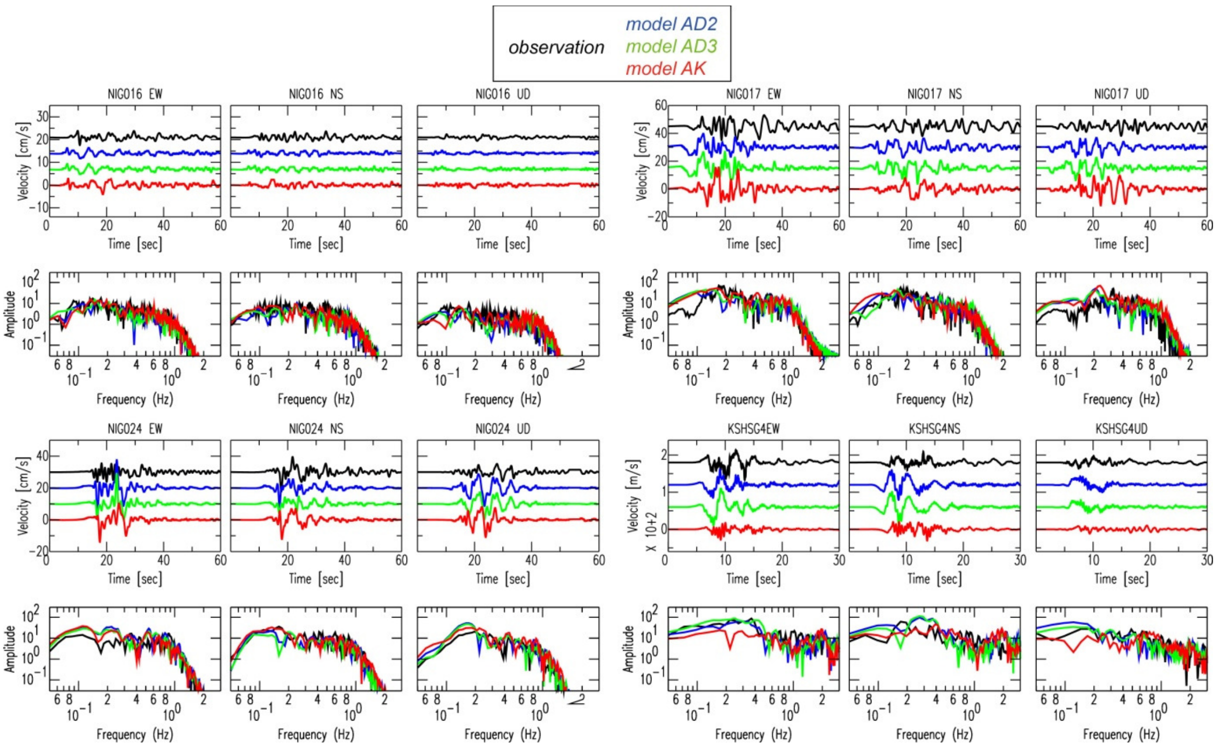

FIG. 4. The comparison of the synthetic seismograms for the three components from the three dynamic earthquake models and the observation. For NIG016, NIG017 and NIG024, the seismograms are filtered between 0.1 to 1 Hz. No filter is applied at KSH – SG4. The time zero is taken as the event time 10:13:22.16 (local time).

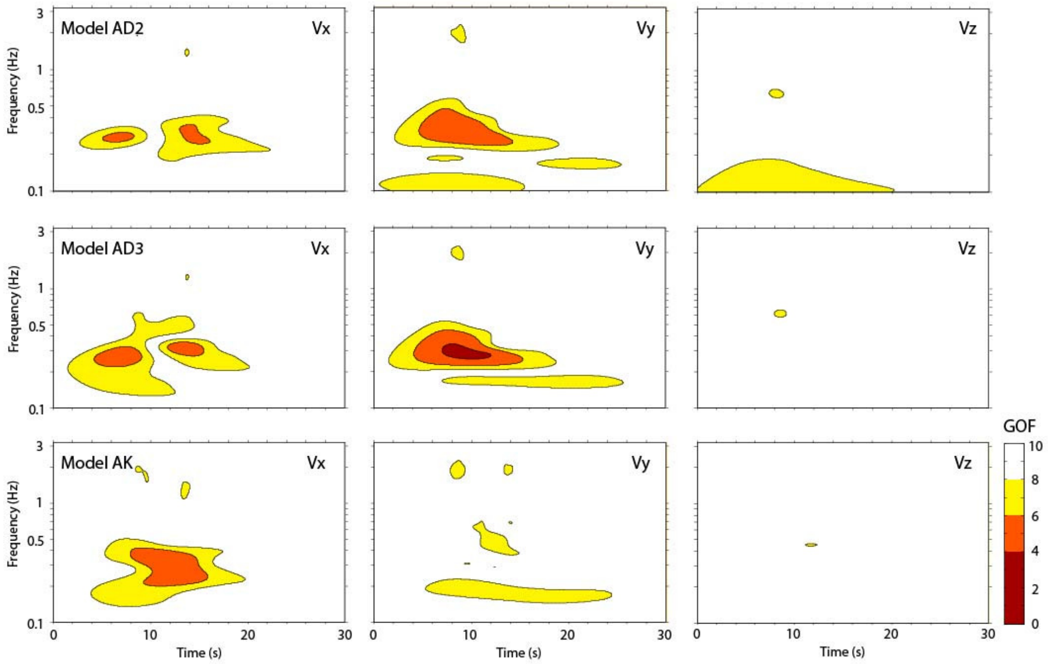

FIG. 5. Time-frequency envelope Goodness-of-Fit (GOF, e.g. [37]) between each synthetic seismogram and the observation at KSH-SG4 (See FIG.4.). The component (x,y,z) represents (EW, NS, UD), respectively. GOF scales from 0 (poor) to 10 (excellent).

5. Perspective and Conclusion

This note summarizes the practices of dynamic rupture simulations rather than various scientific questions. Parameter setting is the most important task in the simulations, and then in the consequent ground motion estimations. The way of the parameter presentations here is based on the experiences obtained from several earthquake modelings, and thus coherent with what we observed. However there should be always other ways to interpret the conditions and/or important uncertainty going with, even if some physical limit is imposed. Therefore for the quantitative applications, a probabilistic approach to generate the parameter sets can be combined [39, 27]. One can even test different interpretations of the fault segmentation models to estimate the possible rupture scenarios. The advantage is to explore not only the variation of the scenarios, but the upper limit of the severest one based on the mechanics, and this cannot be brought by kinematic scenarios or other standard seismic hazard assessment approaches.

There have been some discussions on the ground motions calculated from the dynamic rupture scenarios in terms of the empirical ground-motion prediction equations (GMPEs) [35, 40]. The dynamic-based simulations are consistent with the GMPEs in different factors (PGV, response spectra, etc.) by properly setting a stress drop. It should be remarked that variation observed in the synthetic ground motions are important, as big as a standard deviation of the GMPEs, although propagation and site effects are simplified or ignored. This is because the receivers are ideally and densely distributed in the simulations to detect the wide variation of the ground motions in space. The variations in the near field (< 10 km) are difficult to estimate from GMPEs due to the lack of the observations, and we should complete the dynamic-based simulations.

In the framework presented in this note, the outer parameters of the earthquake rupture can be explored, without any detail on each small segment, namely low frequency-ground motions can be calculated (coherently up to 1 Hz generally, and incoherently upto a few Hz). In some cases, ones need to calculate more high-frequencies. It is one way to introduce very random heterogeneity in the model parameters (e.g. [41]). Otherwise, since we already obtained a brief earthquake scenario, we can combine kinematically high-frequency components. It is proposed [42] to modify the slip distribution of the dynamic rupture simulation so as to be more heterogeneous as like so-called “k-2” model [43]. This is much more convenient way to test many stochastic scenarios than to calculate each dynamic rupture scenario every time. This is also an advantage of the “two-step” simulation procedure as flexible applications.

6. Acknowledgments

This note is summarized according to the invitation of IAEA and the workshop organizer. We thank particularly Dr. Luis Dalguer for this opportunity. This contains many resultants from different past research projects funded in Japan and France, in particular, from DEBATE project funded by Agence Naionale de la Recherches (2009-2012, grant ANR-08-RISK-001). This manuscript is also a contribution to Japanese projects; Grant-in-Aid for Scientific Research B (grant 15H02989) from Japan Society for the Promotion of Science and the Earthquake Research Institute cooperative research program (grant 2013-B-05) (PI: Hiroe Miyake). The calculated results shown as an example are brought at a national supercomputing center (GENCI/CINES-TGCC; grant: 46700). The data for the 2007 Chuetsu-oki earthquake are provided by K-net of National Research Institute for Earth Science and Disaster Prevention (NIED) and by Tokyo Electric Power Company (TEPCO), Japan. FIG. 5 is calculated with the code TF_MISFIT_GOF_CRITERIA written by Kristekova et al. [37].

REFERENCES

[1] DOUGLAS, J., AOCHI, H., “A survey of techniques for predicting earthquake ground motions for engineering purposes”, Survey in Geophysics **29** (2008) 187-220.

[2] IRIKURA, K., MIYAKE, H., “Recipe for predicting strong ground motion from crustal earthquake scenarios”, Pure appl. Geophys. **168** (2011) 85-104.

[3] PEYRAT, S. et al., “Dynamic modeling of the 1992 Landers earthquake”, J. Geophys. Res. **106** (2011) 25467-25482.

[4] AOCHI, H., FUKUYAMA, E., “Three-dimensional nonplanar simulation of the 1992 Landers earthquake”, J. Geophys. Res., **107** (2002) doi:10.1029/2000JB000061.

[5] OLSEN, K. B. et al., “ShakeOut-D: Ground motion estimates using an ensemble of large earthquakes on the Southern San Andreas fault with spontaneous rupture propagation”, Geophys. Res. Lett. **36** (2009) L04303.

[6] AOCHI, H., MADARIAGA, R., "The 1999 Izmit, Turkey, earthquake: Non-planar fault structure, dynamic rupture process and strong ground motion", Bull. Seism. Soc. Am. **93** (2003) 1249-1266.

[7] AOCHI, H., OLSEN, K. B., "On the effects of non-planar geometry for blind thrust faults on strong ground motion", Pure appl. Geophys. **161** (2004) 2139-2153.

[8] AOCHI, H., DUPROS, F., "MPI-OpenMP hybrid simulations using boundary integral equation and finite difference methods for earthquake dynamics and wave propagation: Application to the 2007 Niigata Chuetsu-Oki earthquake (Mw6.6)", Procedia Comptuter Science **4** (2011) 1496-1505.

[9] AOCHI, H. et al., "Finite difference simulations of seismic wave propagation for unerstanding earthquake physics and predicting ground motions: Advances and challenges", J. Phys: Conf. Ser. (2013) 454.

[10] PEYRAT, S., et al., "Which dynamic parameters can be estimated from strong ground motion?", Pure appl geophys. **161** (2004) 2155-2169.

[11] RUIZ, S., MADARIAGA, R., "Determination of the friction law parameters of the Mw6.7 Michilla earthquake in northern Chile by dynamic inversion", Geophys. Res. Lett. **38** (2011) L09317.

[12] AOCHI, H. et al."Spontaneous Rupture Propagation on a Non-planar Fault in 3D Elastic Medium", Pure appl. Geophys. **157** (2000) 2003-2027.

[13] FUKUYAMA, E., MADARIAGA, R., "Integral equation method for plane crack with arbitrary shape in 3-D elastic medium", Bull. Seismo. Soc. Am. **85** (1995) 614-628.

[14] FUKUYAMA, E., MADARIAGA, R., "Rupture dynamics of a planar fault in a 3-D elastic medium: Rate- and slip-wekening friction", Bull. Seism. Soc. Am. **88** (1998) 1-17.

[15] CHEN, X., ZHANG, H."Modelling rupture dynamics of a planar fault in 3D half space by Boundary Integral Equation Method : An overview", Pure appl. Geophys. **163** (2006) 267-299.

[16] TADA, T., "Boundary integral equation method for earthquake rupture dynamics", Fault-Zone Properties and Earthquake Rupture Dynamics (FUKUYAMA, E., Ed.), Elsevier, International Geophysics Series **94** (2009) 217-267.

[17] VIRIEUX, J., MADARIAGA, R., "Dynamic fulting studied by a finite difference method", Bull. Seism. Soc. Am. **72** (1982) 345-369.

[18] OLSEN, K. B., et al., "Three-dimensional simulation of a magnitude 7.75 earthquake on the San Andreas fault", Science **270** (1995) 1628-1632.

[19] GRAVES, R., "Simulating seismic wave propagation in 3D elastic media using staggered-grid finite differences", Bull. Seism. Soc. Am. **86** (1996) 1091-1106.

[20] SAENGER, E. H., et al., "Modeling the propagation of elastic waves using a modified finite-difference grid", Wave Motion **31** (2000) 77-92.

[21] CRUZ-ATIENZA, V. M., et al., "3D finite-difference dynamic-rupture modeling along nonplanar faults", Geophysics **72** (2007) SM123-137.

[22] ZHANG, W., et al., "Three-dimensional elastic wave numerical modeling in the presence of surface topography by a collocated-grid finite-difference method on curvilinear grids", Geophys. J. Int. **190** (2012) 358-378.

[23] MADARIAGA, R., "Dynamics of an expanding circular fault", Bull. Seism. Soc. Am. **66** (1976) 639-666.

[24] GUATTERI, M., et al., "Strong ground-motion prediction from stochastic-dynamic source models", Bull. Seism. Soc. Am. **93** (2003) 301-313.

[25] IDE, S., AOCHI, H., "Earthquakes as multiscale dynamic ruptures with heterogeneous fracture surface energy", J. Geophys. Res. **110** (2005) B11303.

[26] HASHIMOTO, C., et al., "Physics-based 3-D simulation for earthquake generation cycles at plate interfaces in subduction zones", Pure appl. Geophys. **171** (2013), 1705-1728.

[27] AOCHI, H., ULRICH, T., "A probable earthquake scenario near Istanbul determined from dynamic simulations", Bull. Seism. Soc. Am. **105** (2015) 1468-1475.

[28] AOCHI, H. et al., "Effect of normal stress during rupture propagation along non-planar fault", J. Geophys. Res., **107** (2002) 2038.

[29] AOCHI, H., KATO, A., "Dynamic rupture of crosscutting faults: A possible rupture process for the 2007 Mw6.6 Niigata-ken Chuetsu-Oki earthquake", J. Geophys. Res. **115** (2010) B05310.

[30] AOCHI, H. et al., "Constraint of fault parameters inferred from nonplanar fault modeling", Geoch. Geophys. Geosystems **4** (2003) 1020.

[31] INTERNATIONAL ATOMIC ENERGY AGENCY, Preliminary findings and lessons learned from the 16 July 2007 earthquake at Kashiwazaki-Kariwa NPP, Mission report, V.1, International Nuclear Information System **40** (2007) RN40010606 (accessible from https://www.iaea.org/inis/).

[32] IRIKURA, K., "Lesson from the 2007 Niigata-ken Chuetsu-oki earthquake on seismic safety for nuclear power plant", Bull. Japan Asso. Earthq. Eng. **7** (2008) 25-29 (in Japanese).

[33] AOCHI, H., et al., "Finite difference simulations of the seismic wave propagaion for the 2007 Mw6.6 Niigata-ken Chuetsu-Oki earthquake: Validity of models and reliable input ground motion in the near field", Pure appl. Geophys. **170** (2013) 43-64.

[34] SEKIGUCHI, H., et al., "3D subsurface structure model of the Niigata sedimentary basin", Geological Survey of Japan/AIST annual report on active fault and paleoearthquake researches **9** (2009) 175-259 (in Japanese with English abstract).

[35] AOCHI, H., DOUGLAS, J., "Testing the validity of simulated strong ground motion from the dynamic rupture of a fault system, by using empirical equations", Bull. Earthq. Engineering **4** (2006) 211-229.

[36] OLSEN, K. B., MAYHEW, J. E., "Goodness-of-fit Criteria for Broadband Synthetic Seismograms, With Application to the 2008 Mw5.4 Chino Hills, CA, Earthquake", Seism. Res. Lett. **81** (2010) 715-723.

[37] KRISTEKOVA, M., et al., "Time-frequency misfit and goodness-of-fit criteria for quantitative comparison of time signals", Geophys. J. Int. **178** (2009) 813-825.

[38] AOCHI, H., M. YOSHIMI, "Seismological asperity from the point of view of dynamic rupture modeling: the 2007 Mw6.6 Chuetsu-Oki, Japan, earthquake", submitted to J. Seismol. (2015).

[39] AOCHI, H., et al., "Estimating rupture scenario likelihood based on dynamic rupture simulations: the example of the segmented Middle Durance fault, southeastern France", Geophys. J. Int. **165** (2006) 436-446.

[40] BEAUMANN, C., DALGUER L. A., "Evaluating the computability of dynamic rupture-based synthetic ground motion with empirical ground-motion prediction equation", Bull. Seism. Soc. Am. **104** (2014) 634-652.

[41] SONG, S. G., et al., "Pseudo-dynamic source modelling with 1-point and 2-point statistics of earthquake source parameters", Geophys. J. Int. 196 (2014) 1770-1786.

[42] HERRERO, A., et al., "Hybrid broadband ground motion using both dynamic and stochastic methods: Application to the Central Marmara fault (Turkey)", Seism. Soc. Am. Annual Meeting, Pasadena, USA (2015).

[43] HERRERO, A., BERNARD, P., "A kinematic self-similar rupture process for earthquake", Bull. Seism. Soc. Am. **84** (1994) 1216-1228.